MOISTURE PERMEATION MECHANISM OF LATEX FILMS FILLED WITH PLATELIKE FILLERS

Takashi Kawamukai, Etsuko Ishii, and Hisanori Yagi

Oji Paper Co., Ltd., Specialty Products Development Laboratory, 1-10-6 Shinonome, Koto-ku, Tokyo, Japan 135-8558

ABSTRACT

We have developed a new recyclable moisture-barrier paper that consists of a styrene–butadiene rubber (SBR) latex filled with platelike fillers. The degree of the moisture barrier for the recyclable paper is equal to that of a polyethylene-laminated paper. The mechanism of water vapor permeation is explained by the Maxwell tortuosity effect. Apparently, permeability through the filler-filled latex film is significantly affected by the interface between the latex and fillers. It has been also found that platelike fillers depress the solubility of the barrier film.

The mechanism for permeation of water vapor through a polymer film is usually more complex than that of gases such as oxygen or nitrogen. Many investigators have studied the permeation of gases or vapors through a polymer film *(1–8)*. When water vapor permeates through a polymer film, the water molecules sorb at the entering face and dissolve there. The dissolved water molecules then diffuse through the film and desorb at the exit face. Thus the mechanism of permeation involves both solution and diffusion *(1)*.

If water vapor sorption is Henry type and diffusion follows Fick's law, the solubility S is obtained by dividing the concentration of water vapor c by the partial pressure of penetrant at the interface, and the flux J is proportional to the concentration gradient of water vapor. Similarly, the permeability coefficient P is the production of the solubility parameter S and the diffusion parameter D. These two parameters, S and D, explain the mechanism of permeation. For example, the permeability of a polyethylene film is almost equal to that of a polyester film, but their permeation mechanisms are different. The solubility parameter of polyethylene is much smaller than that of polyester, while its diffusion parameter is larger *(4)*.

Generally, water vapor passes through amorphous region of hydrophobic semicrystalline polymers such as polyethylene, but the vapor cannot pass the crystalline phase *(6, 9)*. Thus, the transmission rate decreases when the crystalline region increases or the when the film is stretched to orient the polymer chains.

Polyethylene-laminated papers are widely used because of their excellent barrier property to water vapor. The mechanism of the barrier is dependent on density, which is determined by the crystallinity of the polyethylene.

In the case of a recyclable barrier paper consisting of paraffin wax and synthetic resin latex, the barrier mechanism is based on wax bleeding to the surface of the coating layer *(10, 11)*. The wax on the surface forms a thin layer with high crystallinity and low solubility. Unfortunately, the surface tends to be slippery due to the wax, and the wax is apt to transfer to contents wrapped by the barrier paper. Because of these problems, barrier films containing wax are not used widely for wrapping paper.

There are many reports about the theory of latex film formation *(12–18)* and the moisture permeability of latex films *(19–22)*. Permeation is dependent on glass-transition temperature *T*g, gel fraction, particle size, copolymers, and hydrophilic low-molecular-weight components *(19)*. It is also influenced by deformation or coalescence of latex particles through the process of film formation and by the presence of hydrophilic components like polymerization initiators or emulsifiers.

We have measured the water vapor transmission rates (WVTR) of 20-µm films of various commercial styrene–butadiene rubber (SBR) latexes. The results ranged from 200 to 1000 $g/m^2 \cdot 24$ h, much higher than for polyethylene-laminated paper, with a typical WVTR value of 25 $g/m^2 \cdot 24$ h.

However, it has been found that a 200-µm SBR film, which was coated about ten times, shows a WVTR of 50 $g/m^2 \cdot 24$ h. We were surprised that the incomplete film, which had many pores or defects and contains many hydrophilic components, had barrier properties on a level with polyethylene-laminated paper.

Application of platelike fillers such as mica or tiny clay enhances barrier property, mechanical strength, and heat resistance of polymer films *(23–28)*. For example, addition of platelike fillers to polyethylene resin decreases the permeability *(26, 27)*. Similarly, nylon nanocomposites that contain montmorillonite clay have higher tensile strength, tensile modulus, flexural strength, and flexural modulus than pure nylon *(28)*.

Platelike fillers include graphite, smekutite, and mica minerals (including muscovite, phlogopite, and sericite). The basic structure of mica is aluminum silicate sheets, which are tetrahedral or octahedral. The sheets are combined by cationic ion such as potassium ion, so they are easy to cleave with the point of potassium ion.

We report the barrier mechanism of moisture-barrier layers consisting of SBR latex and platelike fillers. The results show that their permeability rivals that of a polyethylene-laminated paper. Moreover, because the barrier film is imperfectly formed, the barrier paper can be repulped. The barrier layer also contains no wax, so the surface of the barrier paper does not tend to be slippery *(29, 30)*.

EXPERIMENTAL

Materials

SBR latexes for coated paper [styrene–butadiene–acrylic acid copolymer, solids 48 wt%, *T*g 12°C, gel fraction 83%, average particle diameter 190 nm (as measured by laser diffraction and scattering method)] were selected. The platelike fillers were sericite (a product of Taiwan, 15.6-µm average diameter), phlogopite (a product of Finland, 25.2-µm average diameter), muscovite

(a product of India, 20.8-μm average diameter), calcium carbonate (1.9-μm average diameter), and kaolin (6.6-μm average diameter).

A moistureproof coating color was prepared by mixing the prescribed parts (by weight) of fillers, SBR latex, and water. The mixture was stirred in the laboratory for 30 min. The amount of water used in the makeup of the coating color was 50–52 wt% of total solids.

It was coated on a surface of an unbleached kraft paper sheet (70 g/m^2) by using a mayer bar, to form a dry coating layer in an amount of 25 g/m^2, and then dried in a hot-air-circulation drier at a temperature of 110°C for 70 seconds.

The coating colors were applied to the surfaces of PET (polyethylene–terephthalate) films using a Mayer bar to form a dry coating layer with a thickness of 25 μm. The coating was dried at a temperature of 40°C for 5 min, recoated, and dried again at a temperature of 40°C for 24 h. The coating layers were then removed from the PET films. If we coat at one time to form a coating layer in a thickness of 50 μm, the film will be uneven or have many cracks. Hence, we coated two times. Coating layers were carefully removed from the PET films to avoid extending them. If the thickness of the coated layer is too thin (<30 μm) or drying temperature is too high (>60°C), it is very difficult to remove from PET films. The thickness of the coated layer was calculated from coating weight and density of the layer. The calculation is based on the assumption that the density of coated layers on paper is equal to that of PET films.

Measurement

SEM and TEM of the barrier films

Cross-section pictures of SEM (scanning electron microscopy) were made by the glass intercept method. The pictures showed deformation or coming off of the fillers in the films. Then the films were deposited in the liquid nitrogen, and they were broken in it. The cross section pictures made by that method were successful.

The samples of 40°C-dried SBR films for the picture of TEM (transmission electron microscopy) were cut into 10-nm thicknesses, which is smaller than the particle size of the SBR latex.

Density of the barrier films

The density of films was measured by the sink-and-float method at room temperature in aqueous solutions of potassium bromide. The density of the solutions ranged from 1.01 to 1.60 g/cm^3 in intervals of 0.015–0.020 g/cm^3. The films were dried for three days at 40°C in a desiccator filled with anhydrous calcium chloride. The data are intermediate between floating and sinking point, and the values are an average of three measurements.

Particle size and the thickness

The average particle size was measured by laser-scattering particle-size-distribution analyzer (LA-910 HORIBA, Ltd.). The thickness of fillers was measured by the monoparticulate film method *(31)*. The fillers were treated by chlorotrimethylsilane and dispersed in toluene. The solutions of fillers (1 wt%) were developed on water surface, and then the thickness was obtained from the area of the monolayer on water.

Water vapor transmission rate

The water vapor transmission rate was measured at 40°C and 90% RH under JIS Z0208 "cup method," and the values were average of two measurements. The permeability coefficients were obtained from thickness of moisture-barrier layers or films.

Sorption curves, solubility coefficients, and diffusion coefficients

The contents of absorbed water were obtained by weighing films after standing for 24 hours in a chamber that was set at 40°C for each level of humidity.

The sorption curves were measured by weighing the films in the chamber at 40°C 90% RH, and measurement intervals were from 10 min to 24 h. The weight measurement was done as soon as possible in and out using an electronic microbalance that can weigh to a precision of about 0.1 mg. The values were an average of two measurements. The size of the samples was 105 mm × 105 mm.

The solubility coefficients were calculated from water contents of the films at saturation point of the sorption curves. The unsteady-state diffusion coefficients were determined from the slope of the linear portion of the plot of the sorption curves. The steady-state diffusion coefficients were calculated from the solubility and permeability coefficients.

Tensile strength and elongation

Tensile strength and elongation of the films were measured by a Tensilon-type tensile tester. The samples were stored for 24 h under 20°C at 65% RH or 40°C at 90% RH prior to use.

RESULTS

The cross section of moisture-barrier films

Figure 1 shows a cross section SEM picture of a SBR latex film containing 50 wt% phlogopite. The orientation of the fillers is nearly parallel to the surface, although some fillers are arranged obliquely. We analyzed the picture by a computer to estimate the orientation of platelike fillers and the number of fillers. The average of numbers of fillers was about 23 layers per 100-μm thickness. The numbers were obtained from points of intersection of fillers and the line (thickness direction).

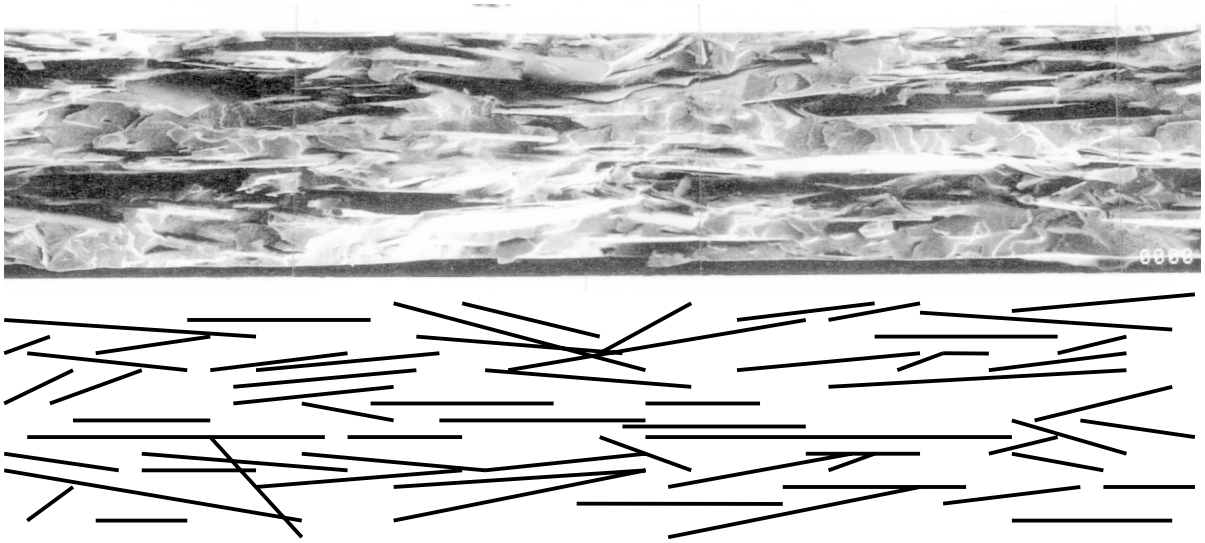

Figure 1. SEM image of cross section of barrier film [SBR latex : muscovite = 50:50 (by weight); film thickness = 50 μm].

Density and porosity

The density of 100% SBR latex film was 1.03 g/cm^3. The porosity of filler-filled films was calculated from the filler density, the unfilled-film density, and the filled-film density. **Table I** shows that the porosity of filled films increases with the volume fraction of fillers. In the case of muscovite, the porosity is 0.87% at 0.136 volume fraction, increasing to 2.39% when volume fraction is 0.269.

It is also found that the porosity depends on the kind of fillers. For example, when the volume fraction is 0.269, the porosity of muscovite is 2.39%, sericite is 2.58%, kaolin is 2.51%, and calcium carbonate is 4.46%.

Aspect ratios of fillers

The aspect ratios of fillers were calculated from average particle size and the thickness. The aspect ratio of sericite was 11.4, that of muscovite was 19.8, and that of phlogopite was 19.9.

Tensile strength and elongation of films

Table II shows the moisture dependency of the tensile strength and elongation of the barrier films. It is found that the strength of the unfilled SBR film does not depend on temperature and humidity. However, elongation for the unfilled SBR film increased from 220% to 315% when the film absorbed moisture.

The strength of the filled films, which is independent of kinds of fillers, was greater than that of the unfilled film, but it decreased greatly when the filled films absorbed moisture under 40°C 90%RH. The tensile elongation, on the contrary, did not change when absorbing moisture.

Film sample	Volume fraction of filler	Filler density, g/cm^3	Theoretical density	Found values of density	Volume fraction of porosity, %
Unfilled SBR film	0	…	…	1.03	0
Filled SBR films					
Muscovite	0.039	2.80	1.10	1.09	0.86
	0.084		1.18	1.15	2.47
	0.136		1.27	1.26	0.87
	0.197		1.38	1.35	2.07
	0.269		1.51	1.47	2.39
	0.356		1.66	1.62	2.37
Phlogopite	0.039	2.84	1.10	1.09	0.92
	0.083		1.18	1.16	1.73
	0.135		1.27	1.26	1.06
	0.195		1.38	1.36	1.62
	0.266		1.51	1.49	2.10
	0.352		1.67	1.62	2.86
Sericite	0.040	2.75	1.10	1.10	0.12
	0.086		1.18	1.16	1.47
	0.138		1.27	1.25	1.41
	0.200		1.37	1.34	2.45
	0.272		1.50	1.47	2.58
	0.360		1.65	1.58	4.17
Kaolin	0.283	2.61	1.48	1.44	2.51
$CaCO_3$	0.258	2.96	1.53	1.46	4.46

Table I. Density of barrier films and volume fraction of porosity.

	Unfilled SBR latex film	Muscovite-filled film (50 wt%)	Phlogopite-filled film (50 wt%)	Sericite-filled film (50 wt%)
Tensile strength, kgf/cm^3				
at 20°C 65% RH	143	286	359	250
at 40°C 90% RH	143	193	204	152
Elongation, %				
at 20°C 65% RH	220	9.1	5.7	8.3
at 40°C 90% RH	315	6.9	8.7	8.1

Table II. Tensile strength and elongation of barrier films.

Water vapor transmission rate and relative permeability

When the basestock is paper, the WVTR values are two-thirds of values of films, as shown in **Table III**. The reason is that the drying temperatures are different. The coated papers are allowed to dry at a temperature of 110°C for 70 sec, while the films are dried at a temperature of 40°C for 24 hours. In the case of paper, the drying temperature is high enough to allow deformation and coalescence of the latex particles. Consequently, defect structures of the barrier layer on the paper, such as voids, pores, and cracks, greatly decrease compared with the films. The TEM observation indicates that the barrier film has many defects or voids between SBR particles, but the paper does not have clear defects or boundary of the particles. It is considered that the decrease of the defect structure enhances the barrier property for the coated papers.

			Barrier papers		Barrier films	
Film sample	Filler content, wt%	Volume fraction of fillers	WVTR, $g/m^2/day$	Relative WVTR	WVTR, $g/m^2/day$	Relative WVTR
Unfilled SBR film	0	0	96	1.00	119	1.00
Filled SBR films						
Muscovite	10	0.039	63	0.66	76	0.63
	20	0.084	47	0.49	60	0.51
	30	0.136	32	0.33	43	0.36
	40	0.197	26	0.27	33	0.28
	50	0.269	22	0.23	24	0.20
	60	0.356	17	0.18	19	0.16
Phlogopite	10	0.039	62	0.65	91	0.77
	20	0.083	49	0.51	85	0.71
	30	0.135	40	0.42	70	0.58
	40	0.195	40	0.42	53	0.45
	50	0.266	36	0.38	43	0.36
	60	0.352	29	0.30	40	0.33
Sericite	10	0.040	66	0.69	86	0.72
	20	0.086	54	0.56	73	0.61
	30	0.138	49	0.51	72	0.61
	40	0.200	52	0.54	73	0.61
	50	0.272	58	0.60	66	0.55
	60	0.360	56	0.58	64	0.54
Kaolin	10	0.042	89	0.93	…	…
	20	0.090	76	0.79	…	…
	30	0.145	78	0.82	…	…
	40	0.208	83	0.86	…	…
	50	0.283	95	0.99	158	1.33
	60	0.372	95	0.99	…	…
$CaCO_3$	10	0.037	91	0.94	…	…
	20	0.080	84	0.87	…	…
	30	0.130	84	0.88	…	…
	40	0.188	85	0.88	…	…
	50	0.258	81	0.84	143	1.20
	60	0.343	85	0.89	…	…

Table III. WVTR and relative WVTR of barrier papers and films.

Regardless of that difference, the relationship of relative permeability and volume fraction of fillers is in agreement. Relative permeability was obtained supposing permeability of the unfilled SBR latex film is 1. (Relative permeability = Permeability when including fillers / Permeability when including no fillers.)

Figure 2 shows that the relative permeability decreases with an increase in volume fraction of fillers. For example, muscovite shows the lowest relative permeability 0.20 when the volume fraction is 0.27. That means the permeability is one-fifth of that of the SBR film. The fillers of large aspect ratio (muscovite, phlogopite, and sericite) show low permeability. On the other hand, fillers with small aspect ratio (calcium carbonate and kaolin clay) show high relative permeability in the range of 0.8–0.9.

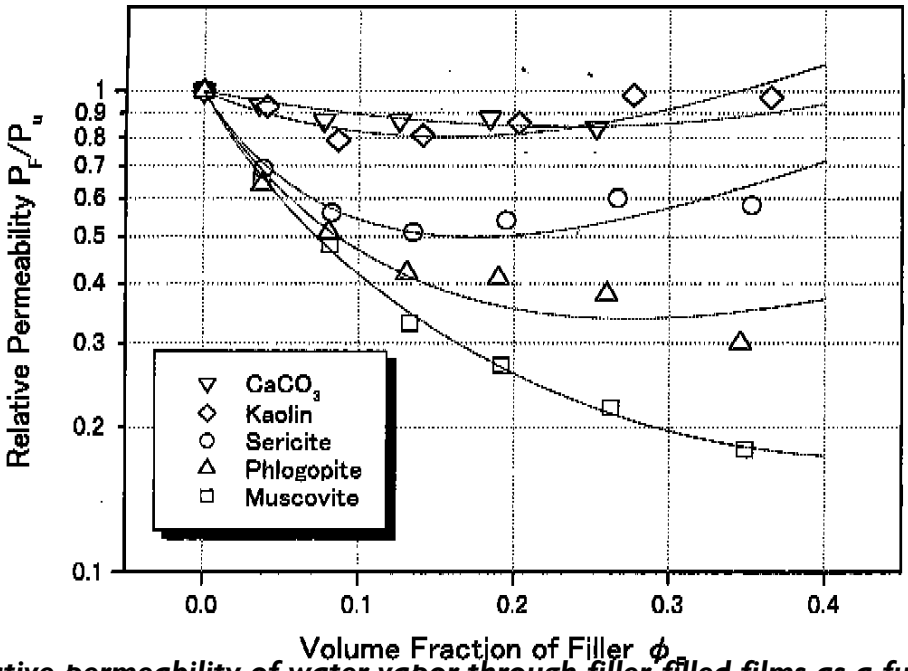

Figure 2. Relative permeability of water vapor through filler-filled films as a function of filler volume fraction.

Water vapor sorption isotherms and sorption kinetics curves

As shown in **Figure 3**, the water vapor sorption isotherms for the SBR film and the muscovite-filled film are type 3 of Brunauer classification *(2)*. The water concentration of the filler-filled film is 0.005 g/cm^3 at 70% RH (vapor pressure = 3.3 cm Hg), but it is 0.015 g/cm^3 at 90% RH (vapor pressure = 5.0 cm Hg).

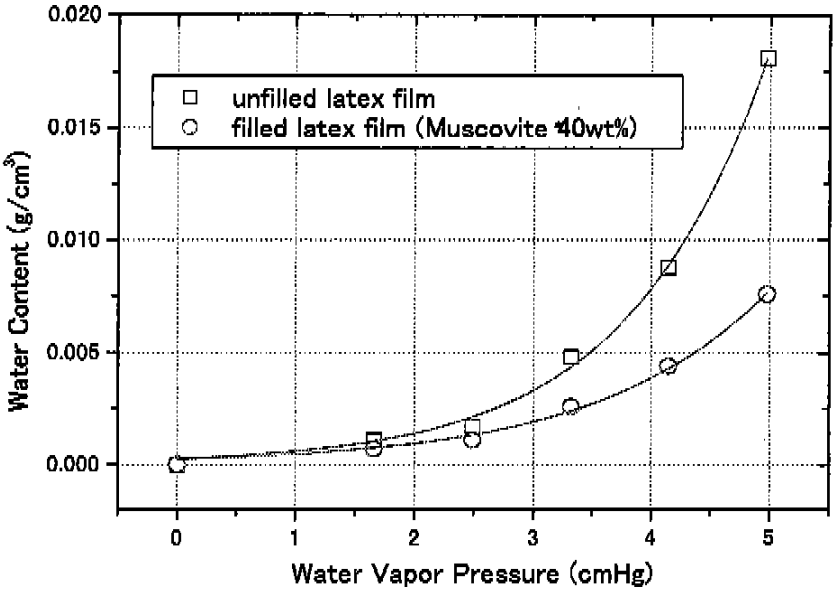

Figure 3. Water vapor sorption isotherms at 40°C.

As seen in **Figure 4**, the absorption curves for the SBR film and the filled film are not in agreement with their desorption curves. The absorption rate is faster than the desorption rate, which means that the diffusion in these films does not perfectly follow Fick's law.

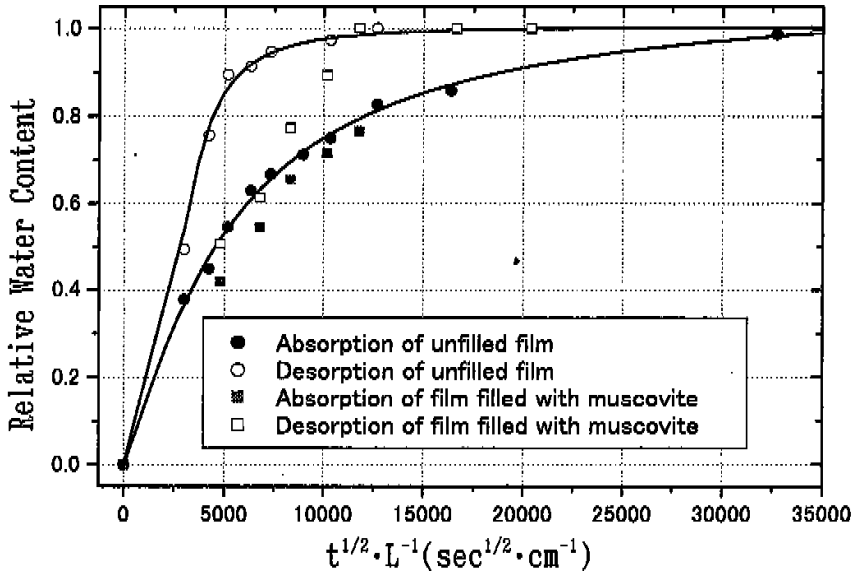

Figure 4. Sorption kinetic curves of unfilled SBR film and SBR filled with muscovite.

Figure 5 shows absorption curves of barrier films at various levels of filler fraction in the film. At short times, all of their plots yield straight lines with the same slope (slope = $2(D/\pi)^{1/2}$), which is readily solved for the diffusion coefficient *D*. Saturated amounts of water absorption decrease linearly with an increase in filler fraction. It is interesting to note that saturated amounts decrease gradually with time.

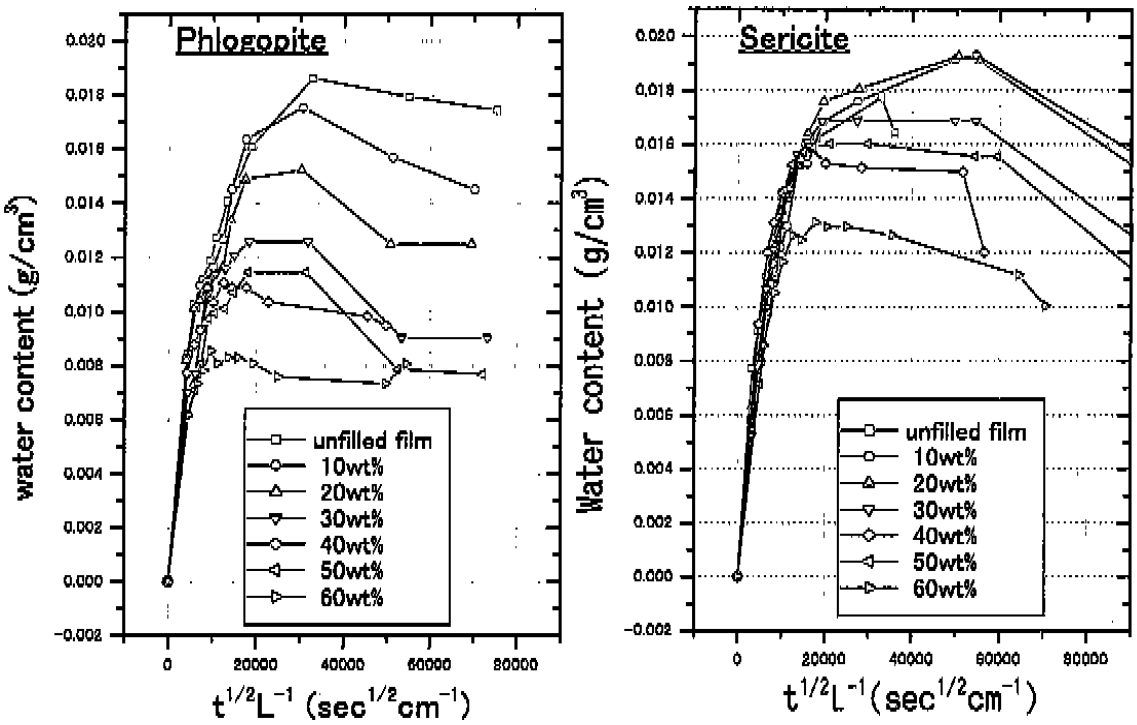

Figure 5. Absorbance curves of SBR latex films filled with phlogopite (left) or sericite (right).

Table IV shows coefficients for permeability, unsteady-state diffusion, steady-state diffusion, and solubility. The solubility coefficients of a steady state are deduced from amounts of water vapor absorption after 24 hours. The diffusion coefficients of a steady-state D_s are obtained by dividing permeability by the solubility coefficients. It is found that relative diffusion coefficients (= diffusion coefficient of filler-filled film / diffusion coefficient of unfilled film) decrease with an increase of volume fraction of filler. Minimum relative diffusion coefficients were 0.25 for muscovite, 0.62 for sericite, and 0.68 for phlogopite.

Film sample	Filler content, wt%	Volume fraction of fillers	Permeability, g·cm/cm^2·s·cm Hg 10^{-11}	Diffusion, cm^2/s 10^{-8}		Solubility, g/cm^3·cm Hg 10
				Unsteady state	Steady state	
Unfilled SBR film	0	0	6.9	0.16	1.8	3.80
Filled SBR films						
Muscovite	10	0.039	4.4	0.15	1.4	3.17
	20	0.084	3.6	0.13	1.0	3.44
	30	0.136	2.5	0.13	7.8	3.23
	40	0.197	2.0	0.14	0.57	3.49
	50	0.269	1.4	0.12	0.5	2.85
	60	0.356	1.1	0.06	0.55	2.02
Phlogopite	10	0.039	5.4	0.16	1.5	3.52
	20	0.083	5.0	0.14	1.6	3.06
	30	0.135	4.0	0.19	1.6	2.52
	40	0.195	3.2	0.21	1.4	2.22
	50	0.266	2.5	0.15	1.1	2.30
	60	0.352	2.4	0.16	1.4	1.72
Sericite	10	0.040	5.0	0.16	1.3	3.87
	20	0.086	4.3	0.20	1.1	3.87
	30	0.138	4.3	0.19	1.8	3.39
	40	0.200	4.4	0.29	1.4	3.19
	50	0.272	3.9	0.19	1.2	3.22
	60	0.360	3.9	0.29	1.5	2.63
Kaolin	50	0.283	8.9	0.30	2.4	3.69
$CaCO_3$	50	0.258	7.9	0.37	4.3	1.84

Table IV. Permeability, diffusion, and solubility coefficients of barrier films

Diffusion coefficients D_U at the unsteady state are 0.12–0.30 × 10^{-8} cm^2/s, and they are independent of volume fraction of the fillers, as seen in **Figure 6**.

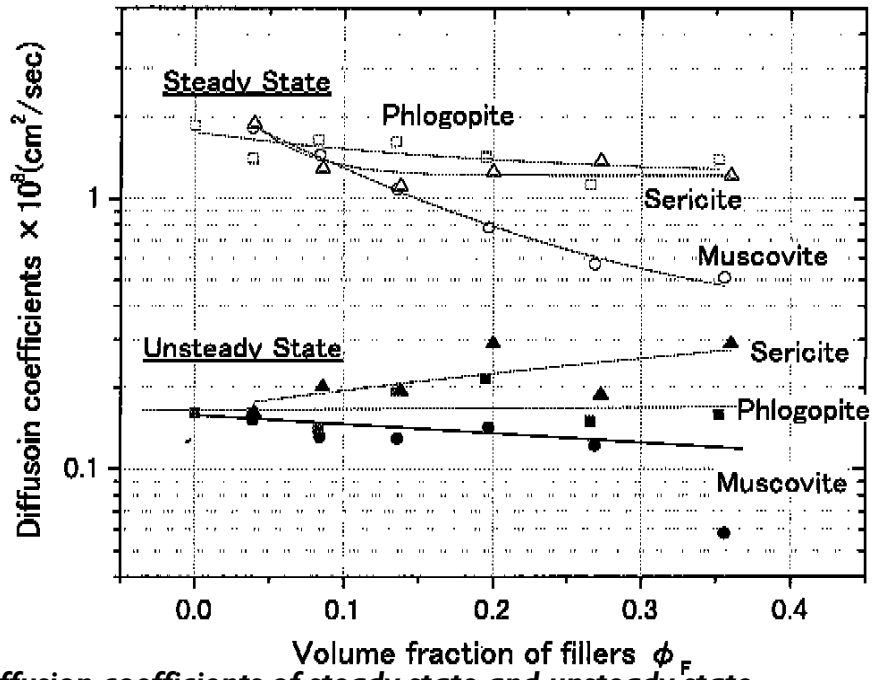

Figure 6. Diffusion coefficients of steady state and unsteady state.

Relative solubility coefficients are obtained by dividing the solubility of filled films by that of unfilled films. **Figure 7** shows that they decrease with an increase of volume fraction of fillers.

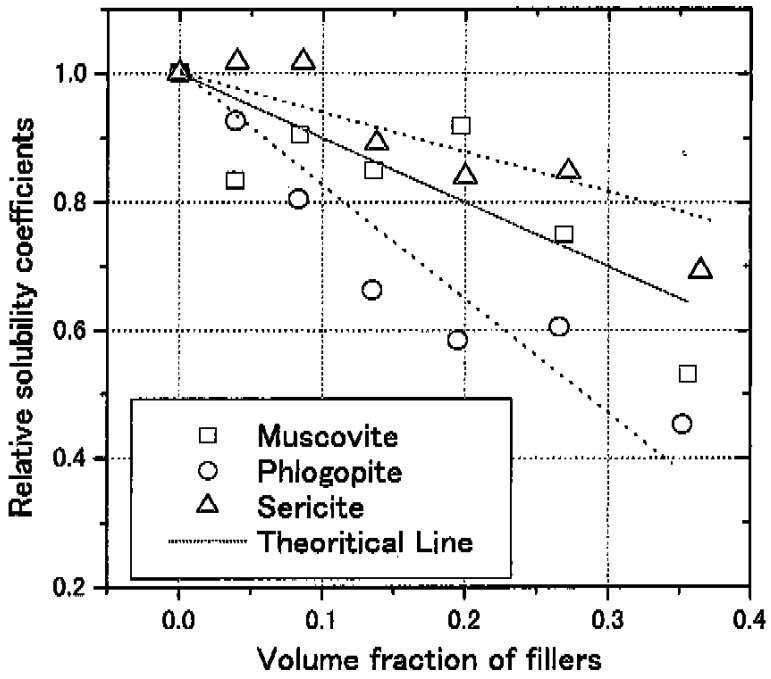

Figure 7. Relative solubility coefficients as a function of volume fraction of fillers.

DISCUSSION

Relationship between film formation of SBR latexes and water vapor sorption

The TEM observation shows that particles of latex deform more or less, but there remain boundaries of the latex particles. This is important, since it is necessary for recycling to maintain the boundaries of latex particles. Coalescence of the particles into a seamless film would reduce the repulpability of the moisture-barrier paper.

The results in Figure 3 showed that water vapor absorption increases linearly with water vapor pressure within the range of 0–3.5 cm Hg, where the absorption follows Henry's law. However, when the pressure is beyond 3.5 cm Hg, the absorption increases exponentially. There seem to be two mechanisms to explain this behavior of the isotherm. First, high water vapor pressure causes water molecules to associate and form clusters in the boundaries of latexes, thus causing an exponential increase in absorption. Second, the hydrophilic components (comonomers, oligomers, and ionic compounds), which tend to absorb moisture at some point of vapor pressure, are located at the boundaries of latexes.

Fick's diffusion requires the desorption rate to be equal to or less than the absorption rate. However, the latex film shows a desorption rate that is greater than the absorption rate. This behavior indicates that the mechanism of the diffusion in latex films — whether filled or not — does not follow Fick's diffusion. In such a case, the water molecules that diffuse through the film constitute clusters that strongly interact with the latex particles. This should affect the diffusion or the structure of the latex film. The counterparts of water molecules on these interactions are comonomer components of latex particles, capillary tubes at the interfaces of the particles, and hydrophilic components such as carboxylic groups, surfactants, and ionic inorganic materials.

The diffusing molecules must push away the interfaces of the coalesced particles, while the film absorbs moisture. On the other hand, when the film desorbs water molecules, they should be expelled by the pressure caused by recoalescence of latex particles. This is the reason why the absorption rate is slower than the desorption rate.

Elongation of the unfilled latex film increased significantly when the temperature and relative humidity were changed from 20°C 65% RH to 40°C 90% RH (Table II). This behavior suggests that solute water molecules plasticize the latex film. The plasticization should occur inside the SBR latex particle or in the highly polar boundary zones between the particles. It is considered that the moisture absorption is saturated at the point of balance between the hydrophilicity and the swelling power of latex particles. The decrease of water content with time suggests that the swelling power becomes strong and therefore expels water molecules out of the latex film.

Models for the permeability of filled polymer systems

The platelike fillers in the filled latex film are oriented approximately parallel to the plane of the film, as seen in Figure 1. If the fillers are impenetrable to a diffusing water molecule, then the diffusing molecules must go around the filler particles. Thus the permeability of the filled latex film can be explained by the Maxwell tortuosity effect *(32)*. The tortuosity factor τ means the extent of a tortuous path for molecules traveling through a filled film (τ = distance a molecule must travel to get through film divided by the film thickness). If the aspect ratio is defined by dividing the average length of a face of a platelike filler particle by the thickness, the tortuosity factor is expressed as:

$$\tau = 1 + \frac{1}{2}\sigma\phi_F \quad \textbf{(1)}$$

where σ is the aspect ratio and ϕ_F is the volume fraction of the polymer *(32)*.

Then the relative permeability is shown:

$$\frac{P_F}{P_U} = \frac{\phi_P}{\tau} \quad \textbf{(2)}$$

where P_F and P_U are the permeability coefficients of the filled and unfilled films, and ϕ_P is the volume fraction of the polymer *(32)*.

At first, we tried to get the aspect ratios to fit the found values of relative permeability as a function of filler volume fraction with use of the nonlinear fit operation of graph resolution software "Origin ver.5". But this operation produced large errors of calculations (the error factor χ = 0.1–1).

Then a similar operation was repeated for volume fractions ranging from 0 to 15%. The results in **Figure 8** produced small errors of calculations (χ = 0.002). The aspect ratios of the platelike fillers can be obtained from the calculation results. The aspect ratios of muscovite, phlogopite, and sericite were calculated as 23, 20, and 14, respectively. However, the second operation also showed large errors over the whole range of volume fraction (Figure 8).

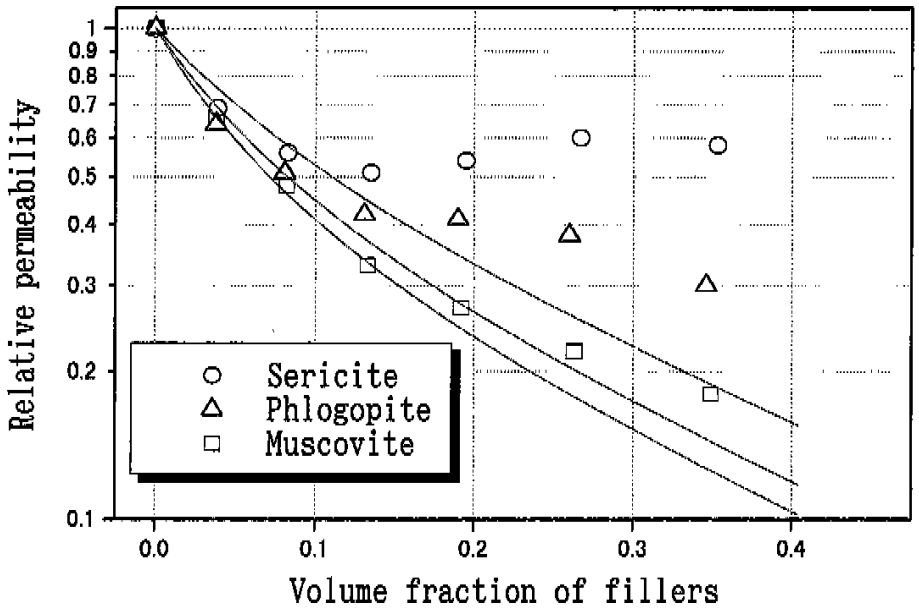

Figure 8. Fitting operations of permeability curves using Eq. 2.

The reason why the found permeability coefficients do not agree with the calculated values is that the porosity at the filler–polymer interface increases with the volume fraction of fillers. This

results in an increase of capillaries (water channels) or pinholes through the film, and these must significantly affect the water vapor permeability.

Nielsen has reported that a permeability coefficient of a filled film is divided into two parts — the interfacial layer and the bulk polymer — provided that the interfacial region affects the permeability *(32)*.

The permeability coefficient is expressed by the sum of that through the interfacial part and through the bulk polymer.

$$P_F = P_1\left(\frac{\phi_I}{\tau^*}\right) + P_2\left(\frac{\phi_P}{\tau}\right) \qquad \textbf{(3)}$$

where P_1 and P_2 are the permeability coefficients of water vapor through the interfacial part and the saturated bulk polymer. P_2 is equal to the permeability P_P of water vapor through the unfilled polymer unless the filler induces changes in the polymer. τ^* is a tortuosity factor for the interfacial part; it may or may not be the same as τ. ϕ_I is the volume fraction of water collected in the interfacial region and ϕ_P is the volume fraction of the polymer. The volume fraction of water dissolved in the polymer is neglected because it is much smaller than that of the polymer.

In the interfacial region, the water molecule must in general go through both the interface and a polymer to get through the film. In this region, reciprocal permeabilities are additive.

$$\frac{1}{P_1} = \frac{\theta_I}{P_I} + \frac{\theta_P}{P_P} \qquad \textbf{(4)}$$

where θ_I and θ_P are the fractional length of diffusion path through the model for the interface and polymer, respectively, $\theta_I + \theta_P = 1$. P_I is the permeability in the interface, which generally would be expected to be much greater than P_P, the permeability in the polymer.
The final equation is obtained from Eqs. 3 and 4:

$$\frac{P_F}{P_P} = \left(\frac{P_I}{P_P\phi_F{}^n + P_I(1-\phi_F{}^n)}\right)\left(\frac{\phi_I}{\tau^*}\right) + P_P\left(\frac{\phi_P}{\tau}\right) \qquad \textbf{(5)}$$

where n is a constant between zero and one, depending on particle shape and orientation ($\theta_I = \phi_F{}^n$, $\theta_P = 1 - \phi_F{}^n$).

We have fitted Eq. 5 by using the aspect ratios that were calculated using the second operation (previously described), where τ^* is the same as τ, and the volume fraction of water collected in the interfacial region is the same as the porosity obtained from the density of the films (Table I). Further, it is assumed that $n = 1$ because the fillers are oriented parallel to the film surface, as seen in the SEM cross sections of the films (Figure 1). Nevertheless, the result of this operation also showed lower permeability than the found values.

Then we assumed that the filler–polymer interfacial layer has no tortuosity effect ($\tau^* = 1$) because the interface region is full of water and does not have barrier property. According to the

operation based on this assumption, the calculation agrees closely with the found values, as seen in **Figure 9**.

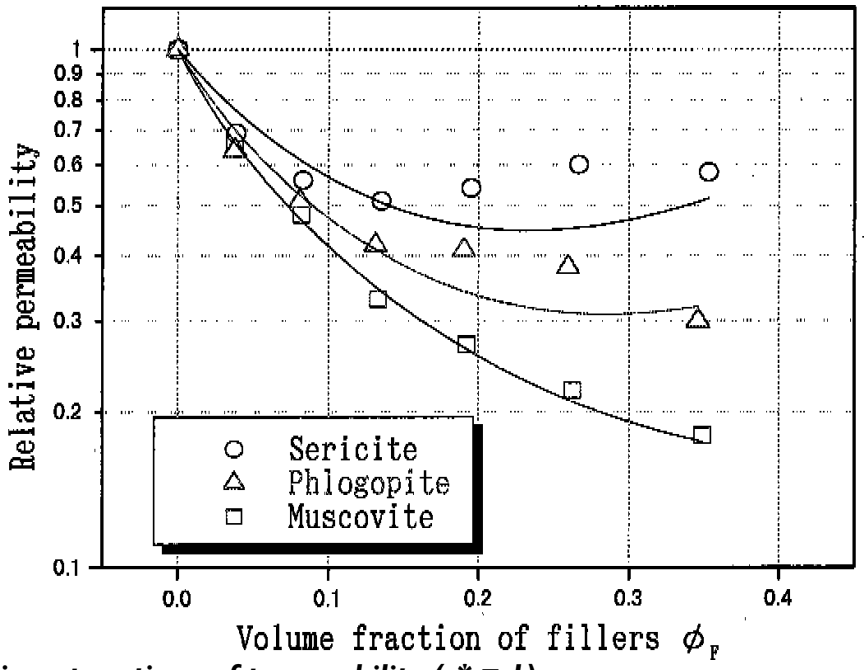

Figure 9. Fitting operations of permeability ($\tau^* = 1$).

The results for tensile strength support the above assumption. When the film absorbs moisture, the strength of the filled film decreases to half or less of the value of the dried film. This behavior suggests that water molecules easily break in the interface of fillers and latex particles, leading to the drop of adhesion force at the interface.

Diffusion and solubility coefficients

Unsteady-state diffusion coefficients, which were determined by the slope of the absorption curves for short times, are independent of filler volume fractions. In the initial diffusion, moisture vapor should go through the interfacial layer between SBR latex particles or platelike fillers and SBR latex. It is considered that the absorption occurs mainly at the latex particle surface, which consists of hydrophilic components, and the rate is much slower than that of latex particles inside, and the absorption amount of the surface is much larger than that of the inside.

It has also been found that the unsteady-state diffusion coefficients depend upon the size of the latex particles. For latex particles with a diameter of 120 nm, the value of the diffusion coefficient is 1.8×10^{-9} cm^2/s, while the 190-nm latex gives a coefficient of 2.5×10^{-9} cm^2/s. This seems to be due to the increase of the particle surface area. The large surface area increases the amount of carboxylic groups at the surface of particles, which must trap water molecules.

Contrary to diffusion at the nonsteady state, at the steady state, water molecules can easily diffuse through the interface region of latex particles. The reason is that the diffusion through the film, which consists of hydrophilic components such as carboxylic groups, generally depends on water concentration. In other words, the diffusion coefficient increases with the concentration of water molecules. In addition, water molecules can diffuse and absorb the interface of the latex

particles and fillers. According to the model for permeability, it is noted that the diffusion through the particle–filler interface should show no tortuosity effect. This argument is consistent with the result that steady-state diffusion coefficients (Figure 6) are larger by about one order of magnitude over nonsteady-state diffusion coefficients, as seen in **Figure 10**.

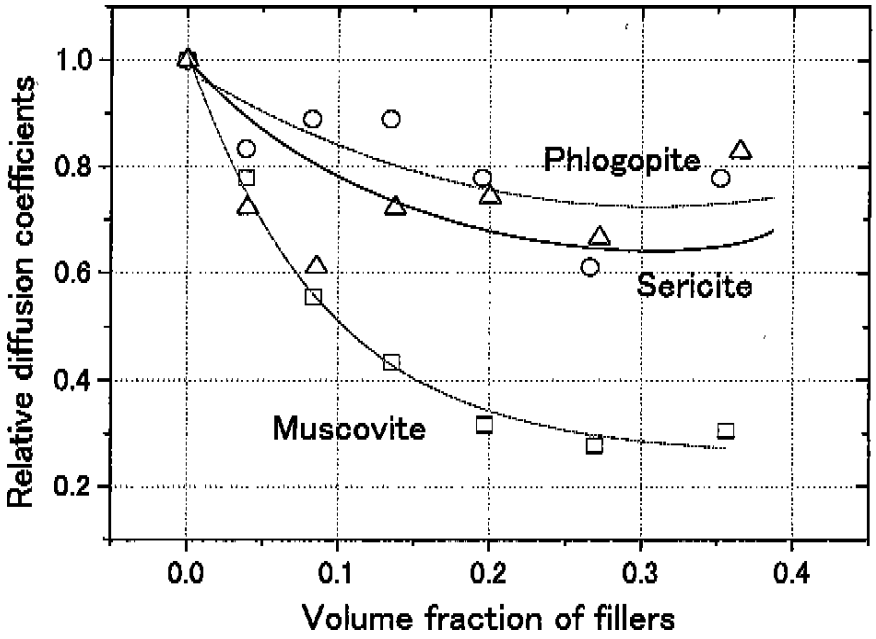

Figure 10. Relative diffusion coefficients at the steady state.

Over longer time periods, the absorption curves show that the amount of water has a tendency to reach a peak and then gradually decrease (Figure 5). This behavior suggests that water molecules in the initial steady state are expelled from the film with the elapse of time. The latex particles, which are dried and contracted, are plasticized and swollen with the process of absorbing water molecules. The swelling decreases the porosities at the interfaces of latex particles or the particles and fillers, thus increasing the pressure of the interface. Consequently, the water molecules are expelled from the film, i.e., the solubility at the steady state decreases with time.

The solubility coefficients as a function of the volume fraction of fillers are shown in Figure 7. In the case of muscovite, it is found that the solubility agreed with the theoretical value, which is based on the assumption that fillers do not absorb water molecules *(33)*. On the other hand, phlogopite shows lower solubility than the theoretical one, although generally a solubility parameter is larger than a theoretical value, as observed for the sericite filler, because the polymer–filler interfaces should absorb excess water. It is suggested that, in the case of phlogopite, there are some factors related to the property of the platelike fillers that decrease the solubility of water. It is considered that the platelike fillers restrict the swelling of latex particles, like plates interposing on an expanding balloon, and as a result, the water solubility of the filled film decreases. From a different point of view, it is possible that the plasticization of the latex film by water molecules improves film formation, thus decreasing film porosity.

Thus, at the steady-state diffusion through a filler-filled film, the barrier property is determined by the balance of solubility, the tortuous effect of the bulk SBR latex, and the diffusion through the interface.

Consequently, the model of permeability through an SBR latex film filled with platelike fillers can be divided into two parts:

1. For the first period of water vapor absorption, the diffusion is mainly affected by the interface of the latex particles. When water molecules reach the interface, they are adsorbed in the hydrophilic components such as carboxylic groups, where the diffusion is smaller by about one order of magnitude over steady-state diffusion. Diffusion is also independent of the volume fraction of fillers because the porosity of the latex film is continuous, thus forming capillary channels.
2. Though the latex particle–filler interface shows no tortuous effect and is full of water vapor at the steady state, the water vapor permeation is smaller than that of the unfilled film because of the decrease of solubility parameters and the tortuous effect of the bulk SBR latex.

CONCLUSION

The objective of this paper was to identify the water vapor permeability properties of SBR latex films filled with platelike fillers. Results show that the permeability is significantly affected by the interface region of the latex particles and fillers. It has been also found that the nonsteady-state diffusion is smaller by about one order of magnitude over steady-state diffusion and does not show a tortuous effect. At the steady state, the solubility decreases with the passage of time, and platelike fillers are likely to depress the solubility of the latex film.

The moisture-barrier wrapping paper, which consists of a SBR latex and platelike fillers, has been used as a recyclable wrapping paper instead of polyethylene-laminated paper.

LITERATURE CITED

1. Vieth, R. W., *Diffusion In and Through Polymers*, Hans Publishers, 1991.
2. Comyn, J., *Polymer Permeability*, Chapman & Hall, London, 1994.
3. Barrer, R. M., *J. Phys. Chem.* 61: 178(1951).
4. Yasuda, H. J. and Stannet, V., *J. Polymer Sci.* 57: 907(1962).
5. Fukuda, M. *et al.*, *Polymer J.* 19(7): 785(1987).
6. Michaels, A. S. and Bixler, H. J., *J. Polymer Sci.* L: 413(1961).
7. Myers, A. W., Meyers, J. A., *et al.*, *Tappi* 44(1): 58(1961).
8. Uchytil, P., Nguyen, Q., *et al.*, *Polymer* 37(1): 93(1996).
9. Alter, H., *J. Polymer Sci.* 57: 925(1962).
10. Yeates, S., Passier, H., *et al.*, Asia–Pacific Conference on Waterborne Coatings, Ink & Adhesives (7th), Kuala Lumpur, 1997, p.74.
11. U.S. pat. 5,358,790 (1994).
12. Wang, Y., Kats, A., *et al.*, *Langmuir* 8: 1453(1992).
13. Imoto, T., *Progress Org. Coatings* 2: 193(1973/1974).
14. Kast, H., *Makromol. Chem. Suppl.* 10/11: 447(1985).
15. Daniels, E. S. and Klein, A., *Progress Org. Coatings* 19: 359(1991).
16. Zhao, C. L. and Wang, Y., *et al.*, *Macromolecules* 23: 4082(1990).
17. Hahn, K., Lay, G., and Oberthur, R., *Colloid Polymer Sci.* 266: 639(1988).
18. Charmot, D. and Guillot, J., *Polymer* 33(2): 352(1992).
19. Richard, J., Mignaud, C., *et al.*, *Polymer Intl.* 30: 431(1993).

20. Vonderhoff, J. W., Bradford, E. B., *et al., J. Polymer Sci. (Polymer Symp.)* 41: 155(1973).
21. Snuparek, Jr., *J. Oil Col. Chem. Assoc.* 55: 1007(1972).
22. Wang, Y., Zhao, C., *et al., J. Chem. Phys.* 95(3): 2143(1991).
23. U.S. pat. 3,663,260 (1972).
24. U.S. pat. 4,082,880 (1978).
25. U.S. pat. 4,528,235 (1985).
26. Busign, C., Lahtinen, R., *et al., Polymer Eng. and Sci.* 24(3): 169(1984).
27. Canova, L. A., *Polyolefins* 10: 145(1997).
28. Miller, B., *Plastic World* October: 36(1997).
29. Kawamukai, T., *et al., Japan TAPPI 65th Pulp and Paper Research Conference Proceedings*, Japan TAPPI PRESS, Tokyo, 1998, p.146.
30. Yagi, H., *29th Summer Seminar Proceedings*, The Society of Fiber Science and Technology, Japan, 1998, p.146.
31. Nishino, M. and Arakawa, M., *J. Soc. Material Sci. Japan* 27(298): 696(1978).
32. Nielsen, L. E., *J. Macromol. Sci. (Chem.)* A1(5): 929(1967).
33. Barrer, R. M., Barrie, J. A., *et al., J. Polymer Sci. Part A* 1: 2565(1963).

Received: March 9, 2000
Accepted: October 19, 2000

This paper was accepted for abstracting and publication in the March 2001 issue of *TAPPI JOURNAL*.

TAPPI Website: www.tappi.org